AIP | Journal of Renewable and Sustainable Energy

Power generation study of luminescent solar concentrator greenhouse

Carley Corrado, Shin Woei Leow, Melissa Osborn, Ian Carbone, Kaitlin Hellier, Markus Short, Glenn Alers, and Sue A. Carter

Citation: Journal of Renewable and Sustainable Energy **8**, 043502 (2016); doi: 10.1063/1.4958735
View online: http://dx.doi.org/10.1063/1.4958735
View Table of Contents: http://scitation.aip.org/content/aip/journal/jrse/8/4?ver=pdfcov
Published by the AIP Publishing

Power generation study of luminescent solar concentrator greenhouse

Carley Corrado,[1] Shin Woei Leow,[2] Melissa Osborn,[1] Ian Carbone,[1] Kaitlin Hellier,[1] Markus Short,[1] Glenn Alers,[1] and Sue A. Carter[1]
[1]*Physics, University of California, Santa Cruz, Santa Cruz, California 95064, USA*
[2]*Electrical Engineering, University of California, Santa Cruz, Santa Cruz, California 95064, USA*

(Received 23 February 2016; accepted 1 July 2016; published online 18 July 2016)

A Luminescent Solar Concentrator (LSC) greenhouse and an identical control greenhouse were constructed with photovoltaic (PV) cells attached to the roof panels of both structures. The placement and types of PV cells used in the LSC panels were varied for performance comparisons. Solar power generation was monitored continuously for one year, with leading LSC panels exhibiting a 37% increase in power production compared to the reference. The 22.3 m^2 greenhouse was projected to generate a total of 1342 kWh per year, or 57.4 kWh/m^2 if it were composed solely of the leading panel of Criss Cross panel design. The LSC panels showed no signs of degradation throughout the trial demonstrating the material's robustness in field conditions. *Published by AIP Publishing*. [http://dx.doi.org/10.1063/1.4958735]

I. INTRODUCTION

As the price of Si photovoltaics (PV) drops, the mounting and support system costs are becoming the limiting factor for installation projects. While the price of Si PV has dropped from >$3/W to as low as $0.34/W in the past four years (http://pv.energytrend.com/pricequotes.html) (Carr *et al.*, 2012), the costs of concrete, racking, and labor experienced less significant change. The development of innovative ways of incorporating PV into buildings using pre-existing structures would greatly increase the access to solar energy by reducing installation costs.

Interest in Building Integrated Photovoltaics (BIPV) is also driven by the desire to mitigate conflicts in land use (Petter Jelle *et al.*, 2012). Availability of cheap Si PV has contributed to the economic viability of establishing massive solar farms to harvest large quantities of clean energy. However, such installations exact a toll on the environment by threatening to alter the habitat of the plants and animals living there (Lovich *et al.*, 2011), (Hernandez *et al.*, 2014). Competition between solar energy production and agricultural productivity is another area of concern as exemplified by the debates surrounding the Williamson Act of 1965, a measure which preserves farmland (Sahagun *et al.*, 2010). Powered by big capital and a re-invigorated industry, the wave of solar energy plants sweeping over the fertile soils of southern California, the Fruit Basket of the United States, has caused a reassessment of land-use values.

The most common BIPV products today have been developed for mounting either on rooftops or on facades (Petter Jelle *et al.*, 2012). Examples of BIPV include PV foils, tiles, modules, and glazing, where silicon wafer and thin films are the most common materials used. Commercial greenhouses, which often span many acres, represent an exciting opportunity to deploy PV technology over large areas with established mounting infrastructure. A representative commercial greenhouse growing operation might occupy 50–100 acres of production under glass and consume significant amounts of electricity for operating deep well water pumps, fans, refrigeration, and lighting. There have been instances that photovoltaics were designed into greenhouses (Sonneveld *et al.*, 2011 and Scognamiglio *et al.*, 2014), but never using luminescent solar concentrators (LSCs) or any type of spectral optimization for plants.

Luminescent Solar Concentrators (LSCs) have the potential for use in greenhouse roof panels to produce electricity while increasing agricultural productivity (Richards *et al.*, 2006;

Van Sark *et al.*, 2008; Sloof *et al.*, 2008; Corrado *et al.*, 2013; Currie *et al.*, 2008; Klampaftis *et al.*, 2009; Leow *et al.*, 2013; and Balaban *et al.*, 2014). An LSC is composed of a solar cell that is optically coupled to a clear, planar waveguide with luminescent dye embedded within the waveguide, or selectively applied to its surface. Incident light is absorbed by the dye, re-emitted, and waveguided to the attached solar cell thereby concentrating light from a larger, planar surface onto a smaller, photoactive area. An LSC has two major advantages over traditional photovoltaics in this particular application. First, the ability to concentrate light reduces the amount of Si PV needed to generate a particular amount of energy; since the waveguiding material is inexpensive, this reduces the cost of the panel. Second, the wave-guiding material is semi-transparent and wavelength selective, making it possible to select only the light that plants do not use for photosynthesis to produce electricity.

Common issues with LSCs are re-absorption losses due to the overlap of the dye's absorption and emission spectra (Saraidarov *et al.*, 2010) and dye stability under solar irradiation (Kinderman *et al.*, 2007; Franklin *et al.*, 2013; and Griffini *et al.*, 2013), with advancements achieved (Slooff *et al.*, 2014). To address the issue of re-absorption, as some have addressed using colloidal nanocrystals instead of a dye (Meinardi *et al.*, 2014 and Coropceanu *et al.*, 2014), we have used a thin dye-embedded matrix to coat one surface of a clear waveguide. Doing so decouples the fluorescent polymer material from the bulk highly transparent low iron glass waveguide and provides photons trapped in the LSC a longer free path before potential re-absorption. Another modification we have made is the switch to face-mounted PV, rather than the traditional edge-mounted design. This supports greater flexibility in design allowing the PV spacing to be adjusted to maximize LSC enhancement and minimize re-absorption (Corrado *et al.*, 2013 and Leow *et al.*, 2013). Dye stability, historically a significant challenge to LSC robustness, is an issue that affects many industries and their combined efforts have seen significant strides forward in improving this issue. For our purpose, a viable solution is just a matter of finding the right mix of UV stabilizers. With these advancements in materials and design, the feasibility of LSC technology for large-scale BIPV installations is lighting up.

The development of a solar panel that may be placed directly above crops with neutral to positive plant response holds significant potential as a new avenue of BIPV, simultaneously providing clean energy and an economic benefit to growers. An important challenge in the development of this technology is to maximize power production without compromise to plant productivity. The development of the material used in this study—in terms of wavelength specificity, dye concentration, and cell density—was done in concert with plant studies through an iterative process (Detweiler *et al.*, 2015). The panel materials fabrication, construction, and layout were discussed in an earlier publication (Corrado *et al.*, 2013). This study represents the first field-test of LSC panels devised in the laboratory, monitoring actual panel performance and reliability over a year. The data collected enabled performance comparison of several panel designs and the quantification of power gain due to light concentration in this cutting edge luminescent solar concentrator design.

II. EXPERIMENTAL METHODOLOGY

Two identical glass greenhouse kits of the dimensions 3.05×7.32 m were purchased from Arcadia Glasshouse and constructed with a North/South orientation, so that 12 windows faced East and another 12 faced West. One of the greenhouses was constructed with LSC electricity-generating roof panels and the other with clear glass including two clear electricity-generating roof panels, as shown in Figure 1. They were constructed in a location without shade and in close proximity to one another while not leading to cross shading.

A circuit diagram illustrating the solar system design is shown in Figure 2. Power from the solar panels was first directed through Tigo Dual Maximizers (MMU), which identified the optimum current and voltage for maximum efficiency in addition to wirelessly reporting data to the Tigo Gateway. The Morningstar maximum power point tracker (MPPT) Charge Controller regulates battery charging to prevent damage from over or under charging. Battery voltage was maintained at approximately 12 V, which was directed through a load switch to power the

FIG. 1. A photograph of the LSC greenhouse (right) and control greenhouse (left) is shown.

Morningstar Relay Driver, Campbell CR1000 Data Logger, Sine Wave Inverter, Cisco Ethernet Switch, and Linksys Router. The inverter powered the Tigo MMU with a 115 V, 60 Hz alternating current. The Morningstar Meter Hub served as a communication hub between the MPPTs and the relay driver. The relay driver can be programmed to activate the power relay running power from the DC line to the fans and refrigerator when the battery is charged to a predetermined level. The Linksys Router, connected to the Cisco Switch, provides internet access through an available wifi to the Tigo MMU, Campbell CR1000, the Morningstar Relay Driver, and

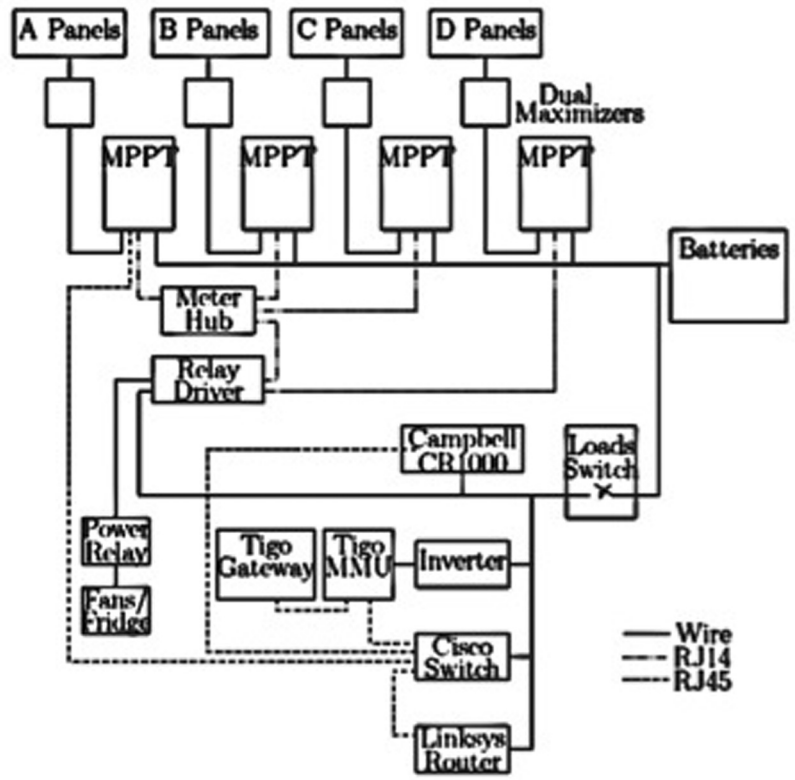

FIG. 2. Circuit diagram showing how power from the panels is maximized, recorded and stored for use on site. Tigo devices were used for maximization and data logging, Morningstar for charge control, Campbell for data logging, and Cisco for communications.

MPPTs. The Tigo MMU reports data on panel voltage, current, and power while the Campbell CR1000 is connected to various data recording devices of which the radiometers were used to determine efficiencies. The three radiometers were positioned with one angled normal to the ground, and one each facing east and west at the same angle as the panels.

A. Panel design

The LSC panels were constructed according to the optimized methodology as described in the previous publication (Corrado *et al.*, 2013). Guardian UltraWhite low iron glass of dimensions 63 cm × 163 cm (0.865 m^2) was used for the construction of the solar panel windows. The LSC panels were constructed to have 13.9% of the back surface covered in PV cells, the majority of which are monocrystalline Si solar cells with an efficiency of 20%, and dimensions 2 cm × 12.5 cm. The designs were chosen based on the combination of scalability and aesthetic, as well as comparing the highest end most expensive monocrystalline cells on the market to the cheaper, lower efficiency polycrystalline cells.

The most basic layout was composed of 4 rows of 12 adjacent PV cells spaced equidistantly, as shown in Figures 3(a)–3(d). Two panels without the LSC coating were mounted on the clear glass greenhouse for control comparisons (Figure 3(a)). Most of the panels in the LSC greenhouse were of this design. Two LSC panels had their PV cells substituted with edge cells (slightly different shape) with equivalent 20% efficiencies (Figure 3(c)). In addition, another two LSC panels were fitted with polycrystalline Si PV cells of 14% efficiency as opposed to the 20% efficient monocrystalline cells. Finally, there were two panels made using 20% efficient monocrystalline cells but laid out in a CrissCross pattern (Figure 3(d)). All panels were designed to ensure that they had an equivalent cell area coverage. In total, there were 22 electricity-generating panels on the LSC greenhouse.

B. Reliability measurements

The lifetime of the material composing the panels should be at least 20 years in order to justify the high cost of a solar generating roof compared to plain glass. To ensure the stability of the dye embedded in acrylic, a variety of stabilizers were added by the plastic extrusion company. An accelerated UV testing system (Kempe *et al.*, 2010) exposed the LSC materials to 84 h of irradiation at 25 suns equivalent to UV-A at 65 °C and 100% humidity for each year of outdoor exposure simulated. Figure 4 shows the performance reliability results of luminescent material with varied stabilizers labeled (a)–(d). The luminescent material with Stabilizer A passed the 20-year UV test and was therefore considered reliable. This material was then used to construct the before mentioned panels.

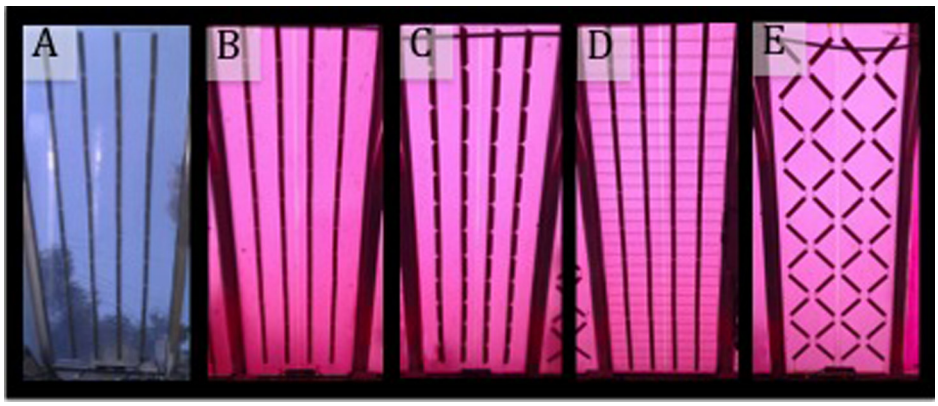

FIG. 3. The five different panel designs are shown: (a) Clear; (b) straight; (c) edge cells; (d) polycrystalline; and (e) criss cross.

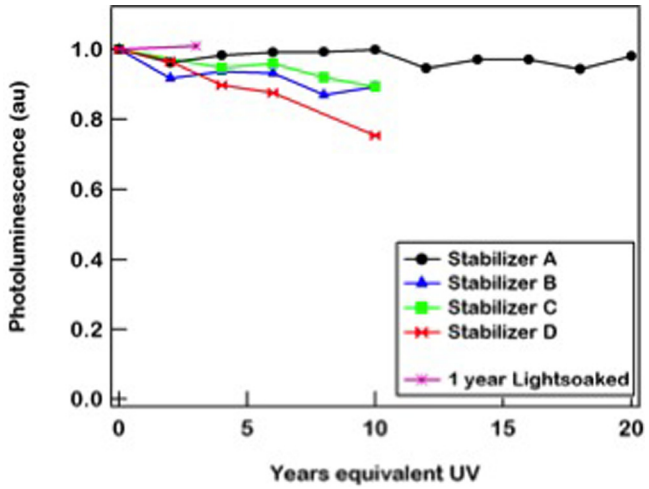

FIG. 4. Accelerated UV-testing of LR-305 dye embedded into acrylic with different UV stabilizers. Stabilizer A showed stability beyond 20 years equivalent of UV and was used in the acrylic used in the greenhouse trial.

In addition to the reliability tests performed in the lab, a sample of the acrylic host matrix was taken from a greenhouse panel and compared with a sample maintained in the lab. The reliability after two years in the field was confirmed by absorbance measurements of the film taken by a UV-Visible Jasco V-670 Spectrophotometer and surface photoluminescence (PL) with a Perkin Elmer LS-45 Luminescence Spectrometer as shown in Figure 5. The relative quantum yield of the greenhouse sample was found using an Ocean Optics Jaz spectrometer connected to an integrating sphere and calculated by the following equation:

$$\varphi_G = \frac{I_G - I_B}{A_G - A_B} \cdot \frac{A_R - A_B}{I_R - I_B} \cdot \varphi_R, \tag{1}$$

where φ is the quantum yield, A is the integrated intensity from 500 nm to 555 nm, and I is the integrated intensity of the sample from 556 nm to 800 nm. The subscripts G, R, and B represent the greenhouse sample, the reference (lab) sample, and a blank sample, respectively.

As seen in Figure 5, the sample taken from the greenhouse exhibits slightly higher absorbance and PL than our reference lab sample; following this observation, several samples from

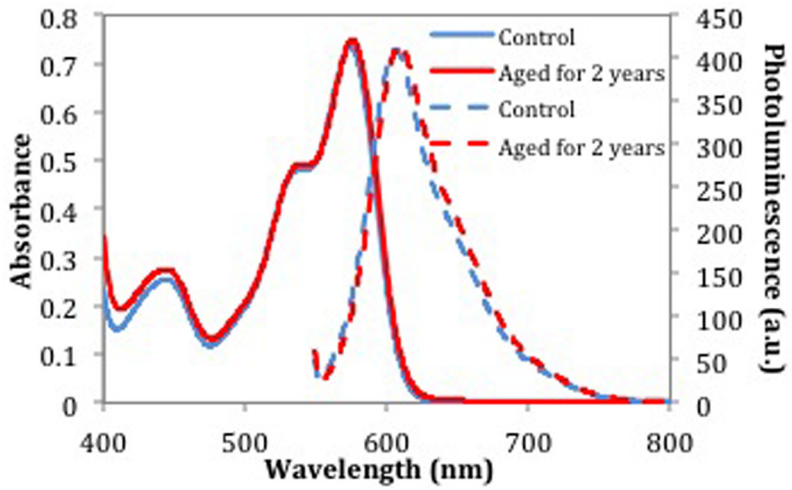

FIG. 5. The absorbance spectra (solid line, left axis) and photoluminescence emission spectra (dashed line, right axis) of the dye at the start of greenhouse trial (blue) and after two years in the field (red) are shown.

one roll of the sheet were tested for absorbance, showing slight variation throughout the sample indicating inconsistency in concentration throughout. As seen in the figure, the slightly higher PL of the greenhouse sample is also redshifted by a few nanometers, indicative of a higher concentration of dye molecules. When compared with the fresh sample with a quantum yield of 85% ± 3% (Corrado, 2013), we found the greenhouse sample falling within error at 84% ± 3%, effectively showing no degradation over time.

I–V curves of the panels were taken at the start of the experiment as well as after two years in the field. The I–V curves of each panel were found to be within error of one another, and hence we present just one plot as a representative of each panel that was tested, and confirmed reliable (Figure 6).

III. RESULTS AND DISCUSSION

A. Panel design comparison

Max power generation was used as the measure of comparison of panel performance. Figure 7 and Table I represent over a year of accumulated data on max power production level in the panels. Data were collected every ten minutes; however, some days show missing data due to communication disruptions between the panels and the measurement hub. Data lost in transmission denotes that the data is a lower estimate on total power production; however, since data for all panels were logged simultaneously, it serves as a suitable method for comparison between the panels. The results of power generation of the four types of panels are shown in Figure 7 and Table I.

The max power data of each type of panel can be used to calculate the enhancement of solar power produced, due to the LSC effect, as a means of comparison of each type of panel. The percentage enhancement is calculated by dividing the luminescent panel power by the reference power and subtracting one.

All enhancement factors were based on comparison to a reference monocrystalline Si solar cell laminated to glass in the same way as the greenhouse panels, with all of the glass masked such that only the cell was exposed to the light. The power generated by the reference cell was then multiplied by 48 (the number of cells in one panel) and used as the benchmark. The leading panels were of the Criss-Cross Design, showing 37% (West) and 32% (East) higher power production than the equivalent of 48 reference cells. This was followed by the Straight Design with an enhancement of 29% (West) and 24% (East). The panels constructed of edge cells showed an enhancement of 17%, and the polycrystalline cells showed an enhancement of 10% only slightly higher than the clear East-facing panel. The clear, control panels had an enhancement of 9% (West) and 8% (East). The enhancement factor of cells attached to a clear glass is a well-established effect due to the scattering of light into the cell from dust and imperfections in the glass.

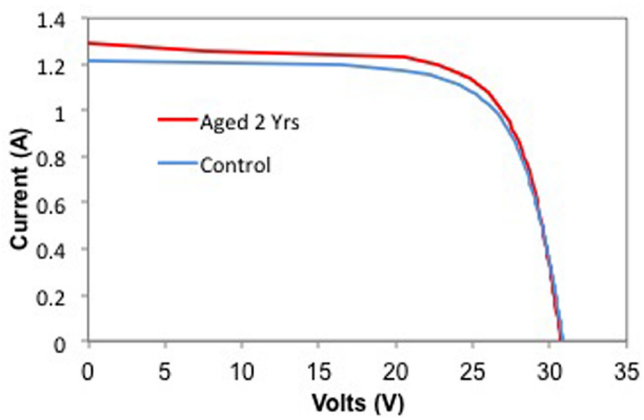

FIG. 6. The I–V curve of one of the panels at the start of the experiment (control) and after two years in the field. The fill factor for this panel is 72%. The other panels exhibit nearly identical I–V curves.

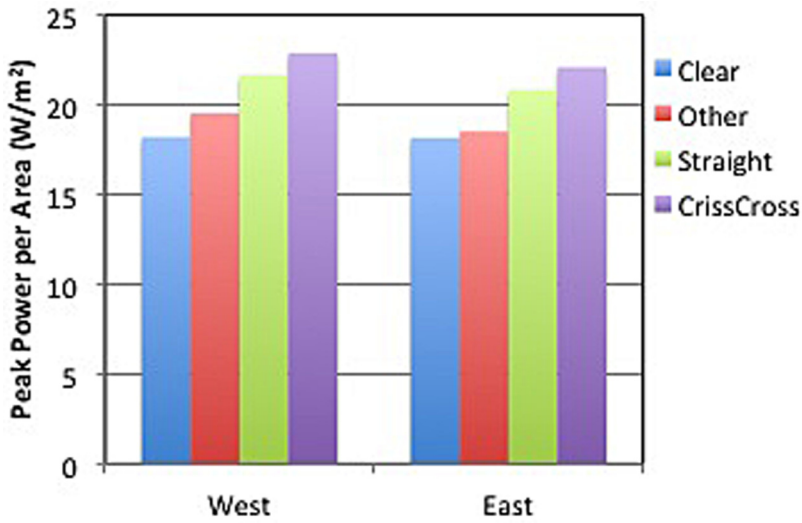

FIG. 7. The comparison of daily peak power over the course of a year produced by panels of varied design for both the West and East sides of the greenhouse. The "other" category on the West-facing side represents the edge cells design, and on the East-facing side represents the polycrystalline Si design.

The polycrystalline Si cells are 14% efficient, compared to the 20% efficiency of the monocrystalline Si cells. Their enhancement factor was calculated by comparison to the reference of monocrystalline Si, which caused their enhancement to appear very low. However, the polycrystalline Si cells cost about ¼ the price of the monocrystalline cells; hence, the possibility exists that the lower efficiency polycrystalline cell could be the most economically viable option. In order to make this determination, an in-depth economic analysis including consideration of installation costs would be necessary, but that is beyond the scope of this paper.

B. Energy generation

It is interesting to compare the actual irradiance data collected onsite to NREL's database in order to give an idea of the variance of actual vs. projected light levels at a given location. The solar irradiance over the course of the experiment (August to July), along with NREL's irradiance for the area, is shown in Figure 8 and Table II. There are some data points that were not recorded because of sensor errors but the majority of the data is intact. Overall, the recorded irradiance averaged over a year was 4.06 kWh/m^2, which is 23% lower compared to

TABLE I. Comparison of panel design performance via averaged daily peak power per area over the course of one year. The enhancement (Enh) was the increase in power compared to that of the reference cell.

Panel design	Power (W/m^2)	Enh
Reference	16.8	…
Clear (W)	18.2	9%
Clear (E)	18.2	8%
Edge cells (W)	19.5	17%
Polycrystalline (E)	18.5	10%
Straight (W)	21.7	29%
Straight (E)	20.8	24%
Criss cross (W)	22.9	37%
Criss cross (E)	22.1	32%

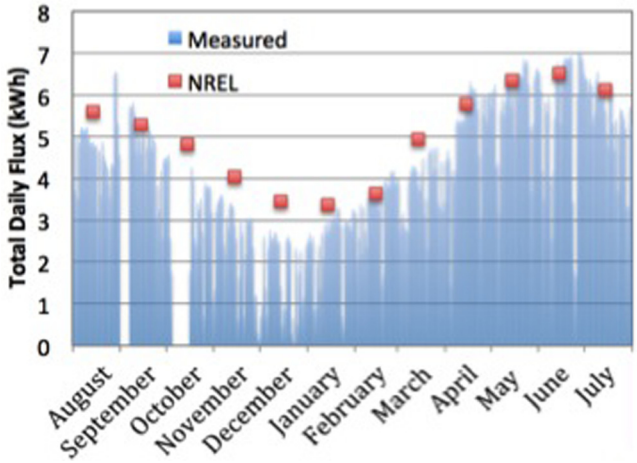

FIG. 8. The total daily flux shows the solar power that was shone onto the greenhouse over the course of the one-year time period of the experiment (blue lines). NREL data corresponding to the same region is compared (red squares).

NREL's 4.99 kWh/m^2. This is likely due to the unusually low amount of light during the winter. The other factor is that NREL's measurements are not from the exact site location as the experiment, and instead averaged over a significant area. The Santa Cruz location was susceptible to fog in the mornings (as can be observed by the lower power generation of the East-facing panels), potentially to a higher degree than the location in which NREL's irradiance data were collected.

The measured efficiencies of the best performing designed LSC panels, Criss-Cross, are compared to the clear panels over the course of a day in Figure 9. The average efficiency of the clear panels was 2.9%, and that of the red panels was 3.8%. Using data from the Criss-Cross panel design and extending that to the whole greenhouse, the potential energy production of the entire greenhouse was extrapolated using the efficiency data and greenhouse irradiance data, and is shown in Figure 10. Overlaid on this projected data is the daily peak power of the Criss Cross panel. This data has gaps due to complications of the wireless communication between the panel's TIGO unit and the database and is hence expected to be lower than the actual peak power, as explained earlier in this section. However, it gives a good general sense of the peak power, and follows the expected trend of correlation with the energy generation of the greenhouse.

TABLE II. The measured irradiance (kWh/m^2) over the course of the experiment is compared to NREL's PV Watts irradiance values. The difference in values is shown as a percentage.

Month	Measured	NREL	% Dif
August	4.73	5.61	19%
September	4.67	5.29	13%
October	3.41	4.81	41%
November	2.45	4.03	65%
December	1.72	3.45	101%
January	2.52	3.36	33%
February	3.32	3.64	10%
March	3.77	4.93	31%
April	5.23	5.78	11%
May	5.87	6.36	8%
June	5.59	6.53	17%
July	5.51	6.12	11%
Average	4.06	4.99	23%

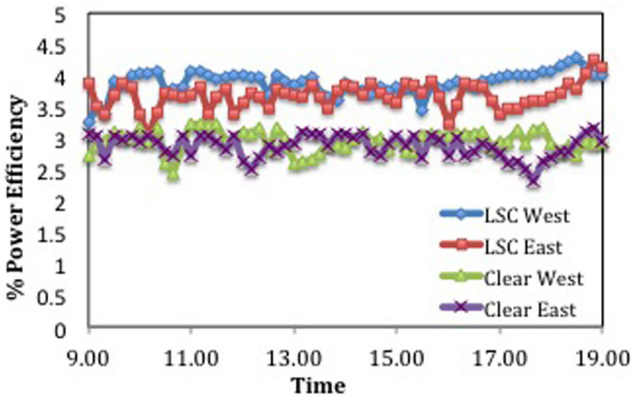

FIG. 9. The efficiency of the East and West-facing criss cross LSC panels and clear panels throughout the day.

The greenhouse was projected to generate a total of 1342 kWh per year, or 57.4 kWh/m^2 if it were composed solely of the leading panel of Criss Cross panel design. The energy output of this greenhouse is subject to weather conditions of the greenhouse location, and hence will vary at different locations. A typical greenhouse in Central California uses 20,000 kWh per 1000 m^2 of greenhouse area for pumps, fans, lighting, and varied other uses. Thus, a greenhouse roof would need approximately 1/3 coverage of LSC electricity-generating panels in order to produce all the electricity consumed in the greenhouse operation.

C. Plant response

The other crucially important component of this technology is the response of plants to the altered light spectrum. The LSC and control greenhouses were designed to monitor plant productivity in addition to the energy production and reliability results presented in this paper. Initial plant trial results have shown neutral to positive effects on plant growth (Detweiler *et al.*, 2015) (more publications in the works), and additional research is needed on an increased variety of plant types. These data will be presented in collaboration with plant physiology experts, and experiments are also underway to better understand the impacts of this technology on plant growth in large commercial growing operations.

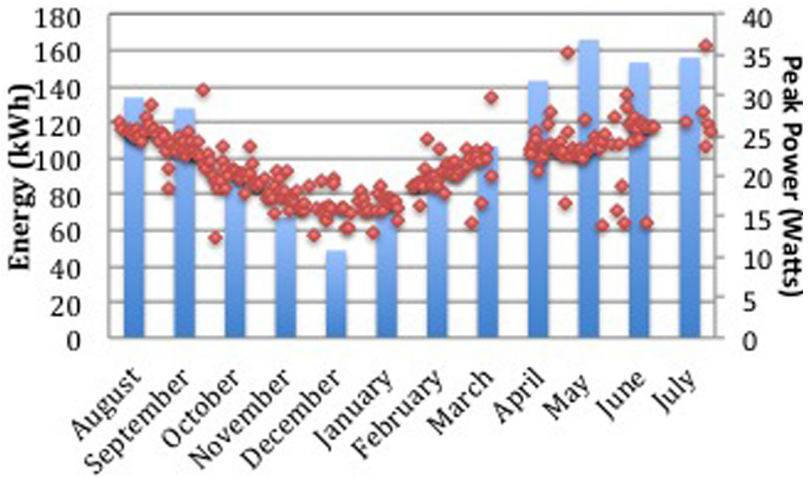

FIG. 10. The daily peak power per m^2 of the criss cross design panel is shown (red diamonds, right axis). The monthly energy generated from the greenhouse (blue bars, left axis) is projected if the criss cross design were used for each of the 24 greenhouse glass panels.

IV. CONCLUSION

LSC panels have been shown to be an effective technology that allows for the harvesting of solar-energy directly above plant growth in greenhouses. The panels rely on organic materials to concentrate light on a relatively small area of thin strips of PV cells. The panels primarily absorb and concentrate specific wavelengths of light that are largely reflected and unused by plants. As a result, these panels have been designed to generate electricity on agricultural land with a neutral or positive benefit to the underlying crops. In addition to enabling the dual use of land for agricultural and energy production, this technology also takes advantage of pre-existing agricultural infrastructure. Using greenhouse structures to host PV technology may significantly reduce installation costs. The results in this paper show that this technology is durable and capable of exceeding the electricity needs of most commercial greenhouse growers. More work is necessary to optimize the panel materials for both energy production and plant productivity. This includes developing luminescent dyes with more targeted absorption and emission properties and improving the geometry of PV cells and other materials to increase the efficiency of the panels. Plant trials and grower feedback will assist in optimizing this technology for plant growth.

ACKNOWLEDGMENTS

This work was supported by the NSF SEES Award No. 1215961 U.S. Department of Energy Grant No. DE-EE0003455 and by the University of California Discovery Grant No. 192864. The research team would also like to thank Derek Padilla for his contribution to building the greenhouse, as well as the UCSC arboretum for providing the location as well as a supportive environment for the project.

Balaban, B., Doshay, S., Osborn, M., Rodriguez, Y., and Carter, S. A., "The role of FRET in solar concentrator efficiency and color tenability," J. Lumin. **146**, 256–262 (2014).
Carr, G., "Sunny uplands: Alternative energy will no longer be alternative," in The Economist, 2012.
Coropceanu, I. and Bawendi, M. G., "Core/shell quantum dot based luminescent solar concentrators with reduced reabsorption and enhanced efficiency," Nano Lett. **14**(7), 4097–4101 (2014).
Corrado, C., Leow, S. W., Osborn, M., Chan, E., Balaban, B., and Carter, S. A., "Optimization of gain and energy conversion efficiency using front-facing photovoltaic cell luminescent solar concentrator design," Sol. Energy Mater. Sol. Cells **111**, 74–81 (2013).
Currie, M. J., Mapel, J. K., Heidel, T. D., Goffri, S., and Baldo, M. A., "High-efficiency organic solar concentrators for photovoltaics," Science **321**, 226–228 (2008).
Detweiler, A. M., Mioni, C. E., Hellier, K. L., Allen, J. J., Carter, S. A., Bebout, B. M., Fleming, E. E., Corrado, C. C., and Prufert-Bebout, L. E., "Evaluation of wavelength selective photovoltaic panels on microalgae growth and photosynthetic efficiency," Algal Res. **9**, 170–177 (2015).
Franklin, J. B., Smith, G. B., and Earp, A. E., "A critical hurdle to widespread use of polymer based luminescent solar concentrators," International Society for Optics and Photonics, Report No. 88250N-88250N, 2013.
Griffini, G., Brambilla, L., Levi, M., Del Zoppo, M., and Turri, S., "Photo-degradation of a perylene-based organic luminescent solar concentrator: Molecular aspects and device implications," Sol. Energy Mater. Sol. Cells **111**, 41–48 (2013).
Hernandez, R. R., Easter, S. B., Murphy-Mariscal, M. L., Maestre, F. T., Tavassoli, M., Allen, E. B., Barrows, C. W., Belnap, J., Ochoa-Hueso, R., and Ravi, S., "Environmental impacts of utility-scale solar energy," Renewable Sustainable Energy Rev. **29**, 766–779 (2014).
Kempe, M. D., "Ultraviolet light test and evaluation methods for encapsulants of photovoltaic modules," Sol. Energy Mater. Sol. Cells **94**(2), 246–253 (2010).
Kinderman, R., Slooff, L. H., Burgers, A. R., Bakker, N. J., Büchtemann, A., Danz, R., and van Roosmalen, J. A., "IV performance and stability study of dyes for luminescent plate concentrators," J. Sol. Energy Eng. **129**(3), 277–282 (2007).
Klampaftis, E., Ross, D., McIntosh, K. R., and Richards, B. S., "Enhancing the performance of solar cells via luminescent down-shifting of the incident spectrum: A review," Sol. Energy Mater. Sol. Cells **93**(8), 1182–1194 (2009).
Leow, S. W., Corrado, C., Osborn, M., Isaacson, M., Alers, G., and Carter, S. A., "Analyzing luminescent solar concentrators with front-facing photovoltaic cells using weighted Monte Carlo ray tracing," J. Appl. Phys. **113**(21), 214510 (2013).
Lovich, J. E. and Ennen, J. R., "Wildlife conservation and solar energy development in the desert southwest, United States," Bioscience **61**(12), 982–992 (2011).
Meinardi, F., Colombo, A., Velizhanin, K. A., Simonutti, R., Lorenzon, M., Beverina, L., Viswanatha, R., Klimov, V. I., and Brovelli, S., "Large-area luminescent solar concentrators based on/Stokes-shift-engineered/'nanocrystals in a mass-polymerized PMMA matrix," Nat. Photonics **8**(5), 392–399 (2014).
Petter Jelle, B., Breivik, C., and Drolsum Røkenes, H., "Building integrated photovoltaic products: A state-of-the-art review and future research opportunities," Sol. Energy Mater. Sol. Cells **100**, 69–96 (2012).
Richards, B. S., "Luminescent layers for enhanced silicon solar cell performance: Down-conversion," Sol. Energy Mater. Sol. Cells **90**(9), 1189–1207 (2006).
Sahagun, L., *Solar Farm Sparks Heated Debate in California's Panoche Valley* (Los Angeles Times, 2010).

Saraidarov, T., Levchenko, V., Grabowska, A., Borowicz, P., and Reisfeld, R., "Non-self-absorbing materials for luminescent solar concentrators (LSC)," Chem. Phys. Lett. **492**(1), 60–62 (2010).
Scognamiglio, A., Garde, F., Ratsimba, T., Monnier, A., and Scotto, E., "Photovoltaic greenhouses: A feasibility solutions for Islands? Design, operation, monitoring and lessons learned from a real case study," in The 6th World Conference on Photovoltaic Energy Conversion, 2014.
See http://pv.energytrend.com/pricequotes.html for Energy Trend PV Spot Price.
Slooff, L. H., Bakker, N. J., Sommeling, P. M., Büchtemann, A., Wedel, A., and van Sark, W. G. J. H. M., "Long term optical stability of fluorescent solar concentrator plates," Phys. Status Solidi A **211**, 1150–1154 (2014).
Slooff, L. H., Bende, E. E., Burgers, A. R., Budel, T., Pravettoni, M., Kenny, R. P., Dunlop, E. D., and Büchtemann, A., "A luminescent solar concentrator with 7.1% power conversion efficiency," Phys. Status Solidi (RRL) **2**(6), 257–259 (2008).
Sonneveld, P. J., Swinkels, G. L. A. M., Van Tuijl, B. A. J., Janssen, H. J. J., Campen, J., and Bot, G. P. A., "Performance of a concentrated photovoltaic energy system with static linear Fresnel lenses," Sol. Energy **85**(3), 432–442 (2011).
van Sark, W. G., Barnham, K. W. J., Slooff, L. H., Chatten, A. J., Büchtemann, A., Meyer, A., McCormack, S. J., Koole, R., Farrell, D. J., and Bose, R., "Luminescent solar concentrators—A review of recent results," Opt. Express **16**(26), 21773–21792 (2008).